Rotational Spectromicroscopy: Imaging the Orbital Interaction between Molecular Hydrogen and an Adsorbed Molecule

Shaowei Li (李少伟), Dingwang Yuan, Arthur Yu, Gregory Czap, Ruqian Wu, and W. Ho

Rotational Spectromicroscopy: Imaging the Orbital Interaction Between Molecular Hydrogen and an Adsorbed Molecule

Shaowei Li[1](李绍巍), Dingwang Yuan[1,2], Arthur Yu[1], Gregory Czap[1], Ruqian Wu[1,*], W. Ho[1,3,*]

[1]Department of Physics and Astronomy, University of California, Irvine, California 92697-4575, USA

[2]College of Materials Science and Engineering, Hunan University, ChangSha, 410082, China

[3]Department of Chemistry, University of California, Irvine, California 92697-2025, USA

A hydrogen molecule can diffuse freely on the surface and be trapped above an adsorbed molecule within the junction of a scanning tunneling microscope. The trapped dihydrogen exhibits the properties of a free rotor. Here we show that the intermolecular interaction between dihydrogen and Mg-porphyrin (MgP) can be visualized by imaging j=0 to 2 rotational excitation of dihydrogen. The interaction leads to a weakened H-H bond and modest electron donation from the dihydrogen to the lowest unoccupied molecular orbital of MgP, a process similarly observed for the interaction between dihydrogen and an adsorbed Au atom.

The nature of the interaction between molecules underlies the understanding of chemistry in diverse fields of chemical synthesis, drug design and molecular electronics [1-3]. The strong covalent bond between molecules has been manipulated and characterized at the single molecule level using the scanning tunneling microscope (STM) [4,5]. The real-space microscopic features possibly resembling the weak intermolecular hydrogen bonds have also been observed using non-contact atomic force microscopy [6], scanning tunneling hydrogen microscopy (STHM) [7], and inelastic tunneling probe (itProbe) [8]. However, the application of real-space visualization of chemical bonding could be enhanced by extending the control and quantifying the intermolecular interactions [9], especially for non-planar geometries between the interacting molecules.

Orbital hybridization and charge transfer are two key mechanisms underlying the interaction between two molecules [4]. The magnesium porphyrin (MgP) molecule can participate as an electron acceptor. In one such instance, a negative ion (MgP$^-$) is formed by tunneling electrons from the STM tip. This single molecule electron transfer is reversible and can be controlled by choosing the bias between STM tip and substrate [10,11]. In contrast, molecular hydrogen can be an electron donor. Dihydrogen cations (H$_2^+$) are formed abundantly in the universe from ionization of neutral hydrogen molecules by cosmic rays. The electron from the occupied σ orbital of neutral H$_2$ (σ$_{\text{H-H}}$) can be transferred to an acceptor if the two molecules have a favorable geometry [12, 13]. Consequently, MgP and H$_2$ can potentially form a donor-acceptor pair and investigation of the interaction between them may reveal insights into the mechanism of intermolecular hybridization and charge transfer.

STM has been used effectively to investigate and manipulate single atoms and molecules. The STM tip and substrate form a nano-cavity in which molecular hydrogen can be trapped at low temperature by

2

van der Waals forces [14-17]. The trapped H_2 is sensitive to its local environment and the spatial variation in the potential energy surface can be quantified by changes in its rotational and vibrational energies [14]. Consequently, we can use the trapped H_2 as a sensor of its environment, such as over another adsorbed molecule to investigate the intermolecular interaction by monitoring the rotational excitation of H_2. The trapping potential moves with the scanning tip. Spatial imaging of the intermolecular interaction between the trapped hydrogen and the underlying molecule can be obtained by rotational spectromicroscopy.

In this letter, we probe the $j=0{\rightarrow}2$ rotational excitation of a trapped H_2 over neutral MgP and anionic MgP^- molecules adsorbed on bi-layer alumina (Al_2O_3) grown on NiAl(110) surface. The Al_2O_3 serves as a decoupling layer to suppress the orbital hybridization between adsorbed molecules and the metal substrate [Fig. 1(a)]. The rotational and vibrational spectra of H_2 trapped above a Au adatom on NiAl(110) are also investigated for comparison to MgP adsorbed on alumina. The rotational and vibrational excitation energies are measured by inelastic electron tunneling spectroscopy (IETS) with the STM. The existence of the rotational spectra and the measured energies suggest that the trapped H_2 behaves like a free three-dimensional (3D) rigid rotor, freely translating and rotating on the surface at 10 K. However, the rotational and vibrational energies and line shapes in the d^2I/dV^2 spectra vary as the trapped H_2 experiences spatially dependent interactions with the underlying surface.

The experiments were performed using a home-built STM operating at 10 K and a base pressure of $3{\times}10^{-11}$ Torr [18]. The preparation of the NiAl(110) surface and Al_2O_3 patches follows previously reported procedures [19]. The Ag tip was electrochemically etched. The clean surface at 10 K was dosed *in situ* with MgP and Au. As hydrogen molecules have limited residence time on the Al_2O_3/NiAl(110)

surface at 10 K, a background pressure of H_2 is kept at 1×10^{-10} Torr throughout the experiment to maintain a constant population of adsorbed H_2 on the surface following an initial dose at 5×10^{-10} Torr for 5 min. A bias voltage V_B is applied to the sample with the tip connected to the current amplifier at virtual ground.

Due to the inhomogeneity of the alumina film grown on NiAl(110), the MgP molecules adsorb in a variety of geometries, including those which can become negatively charged by capturing a tunneling electron from the STM tip [11]. The differential conductance (*dI/dV*) spectra measured over a chargeable MgP show hysteresis during forward and backward scans (ramping V_B up and down). The step-down in the conductance [red vertical arrow in Fig. 1(b)] appears after the onset of the lowest unoccupied molecular orbital (LUMO, 0.5 V for the molecule shown in Fig. 1), indicating that an electron transfer to MgP has occurred through the injection of an electron into the LUMO. The MgP⁻ is reverted back to the neutral molecule by transferring an electron from its singly occupied molecular orbital (SOMO) to the tip at a negative bias, as indicated by the step-down in the conductance when the bias is ramped backward [black vertical arrow in Fig. 1(b)]. Because the STM images closely follow the electronic structure, the topographic images taken at 0.5 V [LUMO, Fig. 2 (a)] for MgP and 0.9 V [singly unoccupied molecular orbital (SUMO), Fig. 2(b)] for MgP⁻ show similar 10-lobes patterns that are in agreement with density function theory (DFT) calculations [20].

After dosing H_2, IETS measurement over the bare alumina surface shows an inelastic excitation signal at 45.1 meV. This signal is attributed to the j=0→2 rotational excitation of molecular hydrogen and has previously been confirmed by isotopic substitution [14, 21]. When the tip is located over one of the prominent lobes in the LUMO of MgP, the j=0→2 rotational excitation energy shifts to 42.0 meV.

The change in rotational excitation energy can be an indicator of a change in the H-H bond length [14]. The downshift of the rotational excitation indicates a stretched and weakened H-H bond, in response to variations in the interaction potential surface. If the tip is moved toward the center of MgP, spectral features in the IETS become progressively weaker and are not resolved directly over the center of MgP. DFT calculations suggest the 3D rotor behavior of H_2 can only exist over the rim of MgP molecule. The rotational motion is suppressed at the center of MgP due to the large anisotropy energy between the vertical and horizontal adsorption geometries of H_2 in the tunnel junction [22], causing the absence of the rotational signal in IETS. Variation in the measured rotational excitation energy is not significant over different outer lobes of a MgP molecule [Fig. 2(c)]. However, variation in the intensity between the lobes indicates that the interaction between hydrogen and MgP is affected by the anisotropy in the adsorption geometry of MgP.

Rotational imaging reveals the role of molecular orbitals in the interaction between H_2 and MgP by measuring the spatial distribution of the second derivative signal d^2I/dV^2 at the rotational energy of 42 meV (Fig. 3). The junction gap is set with 50 mV sample bias and 0.1 nA tunneling current, followed by disabling the feedback and decreasing the bias to 42 mV to record the second derivative rotational signal which is proportional to the second harmonic output of the lock-in amplifier. The rotational image at 42 mV [Fig. 3(e)] shows a multi-lobes pattern that closely resembles the LUMO image [Fig. 3(b)], but is significantly different from the constant-current topographic image taken at 50 mV and 0.1nA (same set point as the rotational image) [Fig. 3(a)]. The spatial contrast can only be observed with the sample bias in resonance with the rotational excitation. The off resonance image at 37 mV is nearly featureless [Fig. 3(d)]. The spatial similarity between the hydrogen rotational image at 42 mV and the MgP LUMO

image at 500 mV indicates that the intermolecular hybridization of MgP and H_2 is dominated by the interaction between MgP LUMO and hydrogen orbitals.

The role of charge transfer between MgP and H_2 is further investigated by rotational analysis of the charged MgP⁻. The j=0→2 rotational excitation signal in the IETS over MgP⁻ is significantly different than over MgP and alumina. The intensity of the rotational excitation signal is lower, possibly because the interaction between MgP⁻ and H_2 is less attractive. The line shape of the rotational feature in the d^2I/dV^2 spectrum at positive bias changes from a peak with a side dip [Fig. 2(c)] into a dip with a side peak [Fig. 2(d)] with the expected behavior at negative bias, which is possibly due to the change in the coupling of the inelastic and elastic tunneling processes or the local variation of surface potential [31, 32]. Aside from the changes in signal intensity and line shape, the excitation energy doesn't change significantly when the tip is moved from alumina to over MgP⁻. The rotational image at 45 mV [Fig. 3(f)] does not reveal clear features within the molecule. The mismatch between the rotational and the SUMO images demonstrates that the singly unoccupied orbital contributes negligibly to the interaction between H_2 and MgP⁻.

The major difference in the interaction with H_2 is that MgP is an electron acceptor while MgP⁻ is an electron donor. In contrast to the SUMO of MgP⁻, the LUMO of MgP readily accepts an electron. In the interaction of H_2 with MgP, electrons in the σ_{H-H} partially transfer to the LUMO of MgP [33]. DFT calculations of the projected density of state (PDOS) [Fig. 3(g)] and charge density difference [Fig. 3(h) and 3(i)] have been performed for the tip-H_2-MgP junction. The Fermi level shifts towards the LUMO when interacting with H_2, compared to the H_2-free junction. Two extra peaks [two vertical arrows in Fig 3(g)] next to the LUMO of MgP confirm the hybridization between the MgP-LUMO and H_2 orbitals.

Calculated charge density difference confirms the electron transfer from H_2 to MgP. The spatial distribution of the transferred charge closely follows the LUMO lobes [Fig. 3(h) and 3(i)].

We study the interaction between H_2 and a single Au atom, another electron acceptor, to further validate H_2 as an electron donor. Electron transfer to a single Au atom to form Au^- has been shown to occur on the surface of NaCl film grown on Cu(100) [34]. The IETS measurement over NiAl(110) shows strong vibrational excitation signal at 15.2 mV for the H_2-surface bouncing mode and a relatively weaker rotational feature at 44.8 mV [Fig. 4]. When the tip is located over an Au atom adsorbed on NiAl(110), the rotational excitation energy decreases to 40.1 meV and the vibrational excitation energy increase to 20.0 meV [Fig. 4(a)]. The increase in the vibrational energy coupled to the decrease in the rotational energy suggests a strengthened H-metal bond and a weakened H-H bond when the tip is positioned over the Au adatom [14, 35]. These results strengthen the conclusion that the H_2 molecule acts as an electron donor and favorably interacts with an electron acceptor.

In summary, hydrogen rotational spectromicroscopy provides a novel approach toward visualizing and quantifying the intermolecular interaction between H_2 over another adsorbed molecule. The ability of the tip to trap a hydrogen molecule as it scans over another adsorbed molecule combined with the sensitivity of the hydrogen rotational excitation recorded by IETS to its immediate environment lead to the implementation of rotational spectromicroscopy. Here we apply this new probe to image the interaction between a hydrogen molecule on top of (instead of next to) a MgP on Al_2O_3 surface. The similarity between the hydrogen rotational image and the LUMO image of MgP suggests that hydrogen orbitals interact with the LUMO of MgP. This conclusion is based on the expectation that the rotational intensity tracks the preferable location of the freely rotating hydrogen over the molecule, and the shift in

the rotational energy reflects the change in H-H bond strength. In contrast, the coupling is not favored between hydrogen and the SUMO of anionic MgP^-. The electron transfer from σ_{H-H} to the empty LUMO in the neutral MgP is critical in this donor-acceptor interaction. The σ-donor nature of H_2 is further confirmed by DFT calculations as well as its interaction with an electronegative Au atom adsorbed on the NiAl(110) surface. The rotational spectromicroscopy extends the study of intermolecular interactions in the direction perpendicular to the surface.

[*]To whom correspondence should be addressed. wilsonho@uci.edu, wur@uci.edu

References:

[1] S. L. Cockrofta and C. A. Hunter, Chem. Soc. Rev. **36**, 172 (2007).

[2] J. K. Gimzewski and C. Joachim, Science **283,** 1683 (1999).

[3] A. E. Reed , L. A. Curtiss , and F. Weinhold, Chem. Rev. **88**, 899 (1988).

[4] H. J. Lee and W. Ho, Science **26**, 1719 (1999).

[5] Y. Jiang, Q. Huan, L. Fabris, G. C. Bazan, and W. Ho, Nature Chem. **5**, 36 (2013).

[6] J. Zhang, P. Chen, B Yuan, W. Ji, Z. Cheng, and X. Qiu, Science **342**, 611 (2013).

[7] C. Weiss, C. Wagner, R. Temirov, and F. S. Tautz, J. Am. Chem. Soc. **132**, 11864 (2010).

[8] C. Chiang, C. Xu, Z. Han, and W. Ho, Science **344**, 885 (2014).

[9] C. A. Hunter, Angew. Chem. Int. Ed. **43**, 5310 (2004).

[10] S. W. Wu, N. Ogawa, and W. Ho, Science **312**, 1362 (2006).

[11] S. W. Wu, N. Ogawa , G. V. Nazin, and W. Ho, J. Phys. Chem. C, **112**, 5241 (2008).

[12] W. L. Yim, J. S. Tse, and T. Iitaka, Phys. Rev. Lett. **105**, 215501 (2010).

[13] C. S. Carr and J. B. Hughes, Environ. Sci. Technol., **32**, 1817 (1998).

[14] S. Li, A. Yu, F. Toledo, Z. Han, H. Wang, H. Y. He, R. Wu, and W. Ho, Phys. Rev. Lett. **111**, 146102 (2013).

[15] J. A. Gupta, C. P. Lutz, A. J. Heinrich, and D. M. Eigler, Phys. Rev. B **71**, 115416 (2005).

[16] C. Weiss, C. Wagner, C. Kleimann, M. Rohlfing, F. S. Tautz, and R. Temirov, Phys. Rev. Lett. **105**, 086103 (2010).

[17] G. Kichin, C. Wagner, F. S. Tautz, and R. Temirov, Phys. Rev. B **87**, 081408 (2013).

[18] B. C. Stipe, M. A. Rezaei, and W. Ho, Rev. Sci. Instrum. **70**, 137, (1999).

[19] X. H. Qiu, G.V. Nazin, and W. Ho, Science **299**, 542, (2003).

[20] J. B. Maddox, U. Harbola, K. Mayoral, and S. J. Mukamel, Phys. Chem. C **111**, 9516 (2007).

[21] F. D. Natterer, F. Patthey, and H. Brune, Phys. Rev. Lett. **111**, 175303 (2013).

[22] See Supplemental Material [url], which includes Refs. [23-30]

[23] G. Kresse and J. Hafner, Phys. Rev. B **47**, 558 (1993).

[24] G. Kresse and J. Hafner, Phys. Rev. B **49**, 14251 (1994).

[25] G. Kresse and J. Furthmuller, Phys. Rev. B **54**, 11169 (1996).

[26] P. E. Blochl, Phys. Rev. B **50**, 17953 (1994).

[27] J. Klimeš, D. R. Bowler, and A. Michaelides, Phys. Rev. B **83**, 195131 (2011).

[28] J. Klimeš, D. R. Bowler, and A. Michaelides, J. Phys.: Cond. Matt. **22**, 022201 (2010).

[29] H. J. Monkhorst and J. D. Pack, Phys. Rev. B **13**, 5188 (1976).

[30] N. Lorente, M. Persson, L. J. Lauhon, and W. Ho, Phys. Rev. Lett. **86**, 2593 (2001).

[31] N. Lorente and M. Persson, Phys. Rev. Lett. **85**, 2997 (2000).

[32] F. D. Natterer, F. Patthey, and H. Brune, ACS Nano **8**, 7099 (2014).

[33] G. J. Kubas, Proc. Natl. Acad. Sci. U.S.A. **104**, 6901 (2007).

[34] J. Repp, G. Meyer, F. E. Olsson, and M. Persson, Science **305**, 493 (2004).

[35] A. Yu, S. Li, G. Czap , and W. Ho, J. Phys. Chem. C, DOI: 10.1021/acs.jpcc.5b00494 (2015).

Figure Captions:

FIG. 1 (color online). Reversible electron transfer to a single Mg-porphyrin molecule interacting with H_2 in a double barrier tunnel junction of the STM. (a) Schematic diagram of a single molecule double-barrier junction with temporarily trapped H_2. The spectroscopic signal arises from the average of many diffusion and trapping processes for H_2. (b) dI/dV spectra measured over a MgP molecule undergoing reversible single electron transfer in the geometry sketched in (a). The inset shows the topographic image of the charged molecule taken with a gap set with $V_B = 1.5$ V and $I_T = 0.1$ nA. The position for recording the dI/dV spectra is marked in the topographic image. The red curve is the dI/dV spectrum taken when the sample bias is ramped from low to high (Forward) while the black curve is taken with the bias ramped from high to low (Backward). The two vertical arrows mark the positions of sudden conductance change during the forward and backward scans, corresponding to the charging and discharging of the molecule, respectively. The onset of the LUMO of MgP is around 0.5 V, and the onsets for the SUMO and SOMO of MgP⁻ are around 0.6 V and −0.5 V, respectively.

FIG. 2 (color online). Rotational spectra of single H_2 molecule interacting locally with Mg-porphyrin measured by STM-IETS. (a-b) Topographic images taken at the onset of MgP LUMO (a) and the onset of MgP⁻ SUMO (b). The set points are $V_B = 500$ mV, $I_T = 0.1$ nA for (a) and $V_B = 800$ mV, $I_T = 0.1$ nA for (b). (c) The IETS spectra of trapped H_2 taken over different positions over MgP and alumina, as marked in (a). The vertical dashed line indicates the energy of $j=0\rightarrow2$ rotational excitation of H_2 measured over position 1 of MgP. For all the spectra, the tunneling gap is set with $V_B = 50$ mV and $I_T = 0.1$ nA, and the sample bias is modulated at 345 Hz and 5 mV rms. The spectra are the result of an

average of 10 scans. (d) The IETS spectra taken under same set point conditions as in (c) for positions over MgP⁻ as marked in (b). The spectra are the result of an average of 50 scans. The vertical dashed line indicate the $j=0\rightarrow2$ rotational excitation of H_2 measured over alumina background.

FIG. 3 (color online). Single molecule rotational imaging. (a) Constant current topographic image of MgP taken at $V_B = 50$ mV, $I_T = 0.1$ nA. (b-c) Topographic images showing the (b) LUMO of MgP imaged at $V_B = 500$ mV, $I_T = 0.1$ nA, and (c) SUMO of MgP⁻ imaged at $V_B = 800$ mV, $I_T = 0.1$ nA. The structure of the molecule is superposed on the images. (d) d^2I/dV^2 images taken at 37 mV which is off-resonance of the j=0→2 rotational excitation energy of H_2. The image doesn't show obvious structure. (e) d^2I/dV^2 image taken at 42 mV on MgP showing the multi-lobes feature, and additionally the overall size of the image closely follows the molecular skeletal structure superimposed in (b) and (c) . (f) d^2I/dV^2 on-resonance image taken at 45 mV on MgP⁻. The image also does not reveal clear structure. (g) Calculated partial density of states (PDOS) of tip-MgP junction (top) and tip-H_2-MgP junction with configuration (*5-d)* in TABLE S1. The calculated image of the LUMO for MgP is shown in the inset. The two new features of MgP states (blue solid peaks) in resonance with H_2 states (red dashed peaks) are indicated by arrows in the bottom panel. (h) top view and (i) side view of the charge density difference in tip-H_2-MgP junction. Yellow region indicates charge accumulation while blue regions indicate charge depletion. The value of isosurface for the charge difference is 0.0004 bohr⁻³. The results repeat in the other three quadrants of the molecule.

FIG. 4 (color online). Spectral shifts over an Au adatom. (a) d^2I/dV^2 spectra of H_2 trapped over NiAl(110) substrate (top spectrum) and an Au adatom (middle spectrum). The $j=0\rightarrow2$ rotational excitation energy of H_2 is 44.8 meV over NiAl(110) substrate and 40.1 meV over Au adatom. The v=0$\rightarrow$1 vibrational excitation energy of the H_2-surface bouncing mode is 15.2 meV over NiAl(110) substrate and 20.0 meV over Au adatom. The d^2I/dV^2 spectra (BK) taken before dosing H_2 and over NiAl (bottom spectrum) is nearly featureless. All the spectra are taken with set point $V_B = 50$ mV, $I_T = 1$ nA. (b) Topographic image of Au adatoms on NiAl(110); Au adatom (marked by dotted box) appears as a small round protrusion. The larger square protrusions are adsorbed MgP molecules. (c) Zoom in topographic image of the Au adatom marked in (b). The set point is $V_B = 100$ mV, $I_T = 0.1$ nA for both (b) and (c).
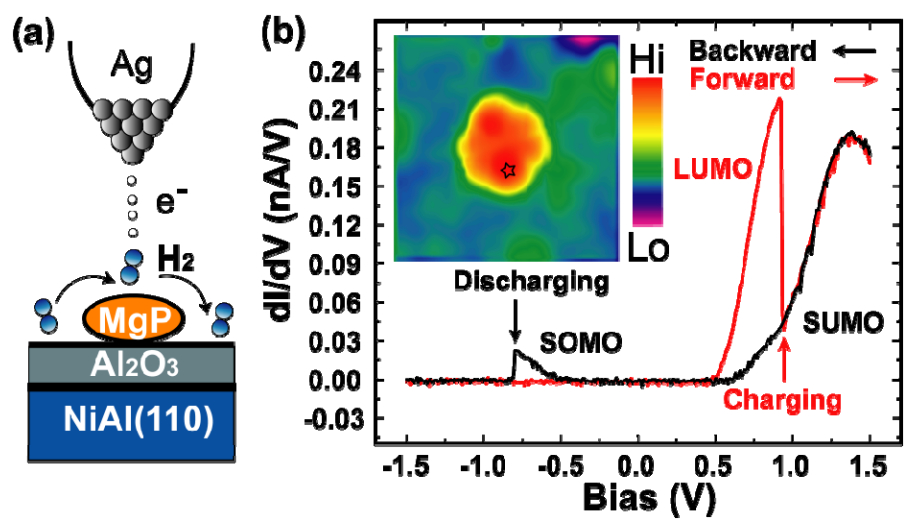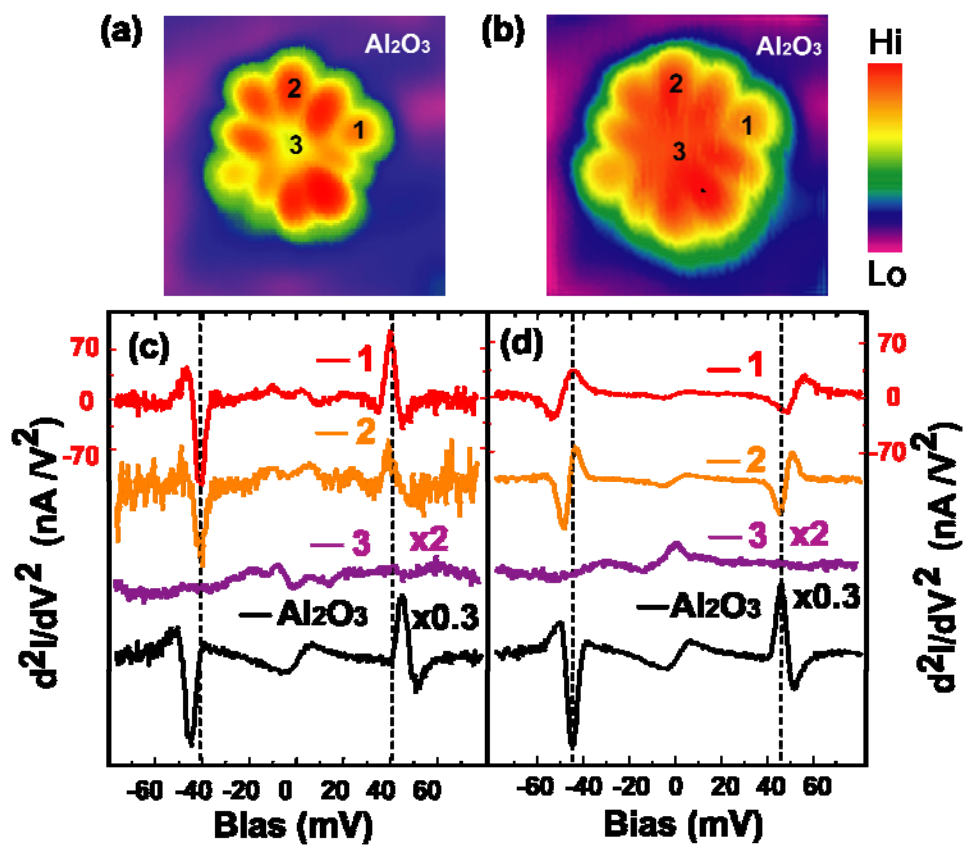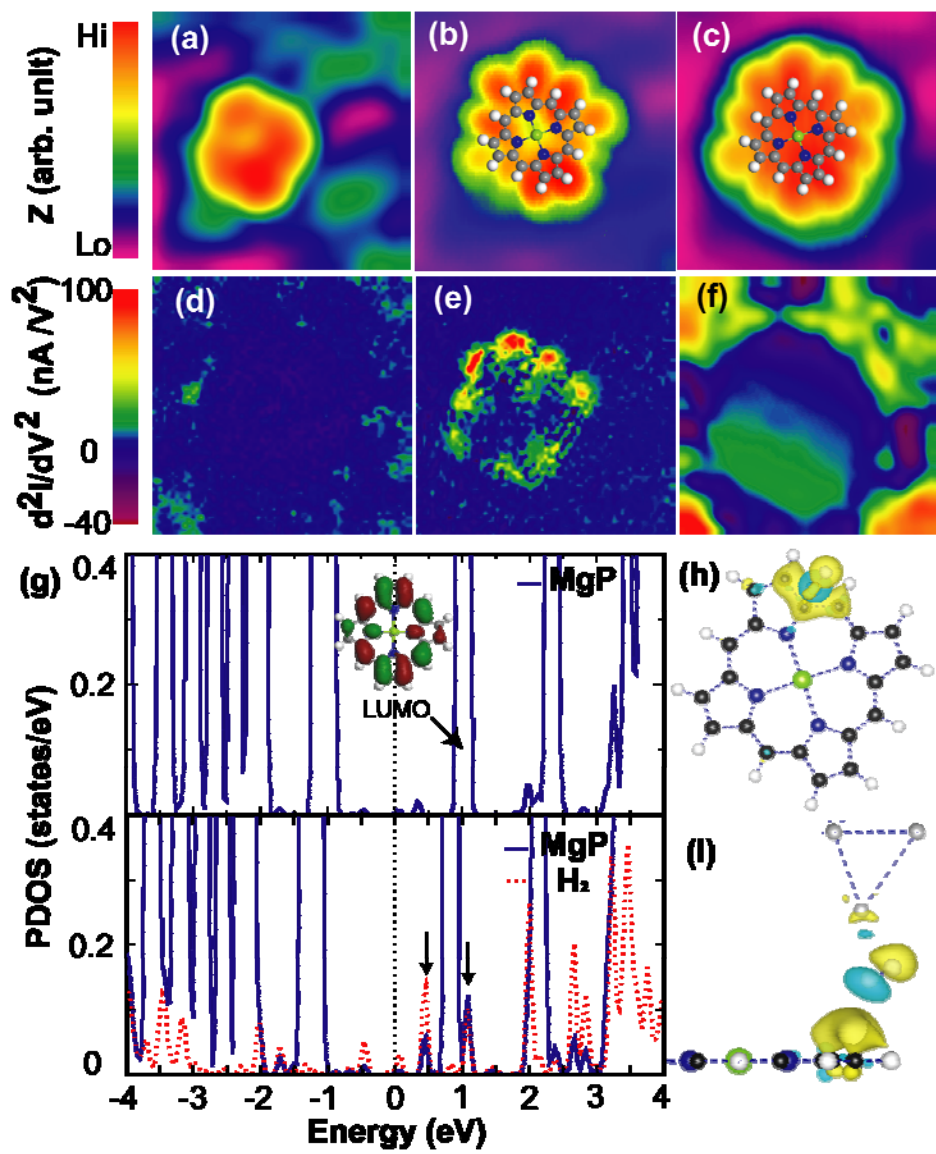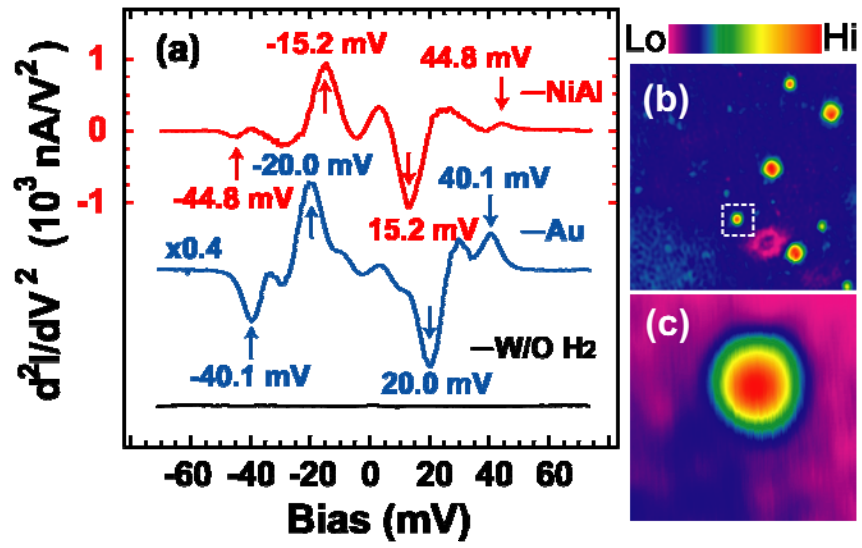
FIG. 1

FIG. 2

FIG. 3

FIG. 4